

## Examination of the Empirical Relationship between High-Resolution Dual-Doppler Wind Profiles and In-Situ Anemometry

R.J. Krupar III<sup>1</sup>, M.S. Mason<sup>1</sup>, W.S. Gunter<sup>2</sup>, and J.L. Schroeder<sup>2</sup>

<sup>1</sup>School of Civil Engineering  
The University of Queensland, St. Lucia 4072, Australia

<sup>2</sup>Department of Geosciences  
Texas Tech University, Lubbock, Texas 79409, USA

### Abstract

This study compares high-resolution dual-Doppler range height indicator (RHI) horizontal wind profiles generated from Texas Tech University Ka-band (TTUKa) mobile Doppler radars and in-situ anemometry mounted on the National Wind Institute (NWI) 200-m tower during a thunderstorm outflow event on 4 June 2012. Preliminary comparisons between the dual-Doppler radar and both the ultrasonic and UVW anemometric wind histories at approximately 50-, 70-, 110-, and 150-m reveal that the 0.4 Hz TTUKa dual-Doppler radar RHI horizontal wind speeds have a positive bias and the magnitude of the mean wind speed percentage difference between the three platforms above 50 m ranges from 2.24% to 4.42%. Time lags between the dual-Doppler radar and anemometric wind histories were noted at each height level and were attributed to the large distance separation between the intersection of the RHI sweeps and NWI 200-m tower. Linear regression models were constructed using UVW wind histories decimated to 0.4 Hz, as well as the dual-Doppler radar RHI horizontal wind speeds for outflow and stratiform regimes. The outflow regime was further segregated into dual-Doppler radar RHI horizontal wind speeds that were greater than or equal to 19 ms<sup>-1</sup> and wind speeds less than 19 ms<sup>-1</sup> to examine the influence of wind shear on the regression fits. The correlation between the two measurement platforms increased with increasing altitude for the outflow regime with wind speeds greater than 19 ms<sup>-1</sup>, while the correlation decreased with increasing altitude for the outflow regime with wind speeds below 19 ms<sup>-1</sup>. This decrease in correlation was attributed to a narrower wind speed range and lack of data at higher elevations. For the stratiform regime, the correlation increased to 70-m, but did not vary significantly over the profile depth when compared with the outflow regimes.

### Introduction

In a recent study by Gunter et al. (2015), two Texas Tech University Ka-band (TTUKa) mobile Doppler radars (Weiss et al. 2009; Hirth et al. 2015) were deployed nearby a triangular, open lattice 200-m tower located at the National Wind Institute (NWI) Reese Technology Center (RTC) field site in Lubbock, Texas. A new coordinated range-height indicator (RHI) scanning strategy was employed to obtain high-resolution dual-Doppler radar RHI horizontal wind speed and direction time histories for comparison with ultrasonic and UVW anemometric wind histories mounted on the NWI 200-m tower in a variety of atmospheric conditions (i.e. clear air, thunderstorm outflow, and snow).

Results from this study revealed that differences between the dual-Doppler radar and mean (i.e. 10-min) anemometer wind histories were strongly influenced by the type of scatterers, especially below 50-m (Gunter et al. 2015). For example, the dual-Doppler radar 10-m mean horizontal wind speeds were on average 15.6% greater than those measured by anemometers during thunderstorm outflow cases. However, little difference was noted between measurement

platforms in clear air and snow at the same measurement height. Above 50-m, the dual-Doppler radar RHI mean horizontal wind histories exceeded the ultrasonic and UVW mean wind histories by only 5%-6% across all atmospheric conditions.

The effect of averaging time on the dual-Doppler radar RHI horizontal wind histories was examined using the clear air data set since it was the longest data record of all cases collected. Coordinated RHI dual-Doppler radar horizontal wind profiles were averaged over 2-, 5-, 10-, 15-, and 30-min time windows and linear regression was employed to evaluate the statistical correlation between the dual-Doppler and anemometric mean wind speed measurements at the 10-, 47-, 75-, 116-, 158-, and 200-m levels. Results showed that as the averaging time and altitude increased, so did the correlation coefficient, *R*. However, it was noted that modulating the averaging time had little influence on the horizontal wind speed biases when compared with a 10-min averaging time window (Gunter et al. 2015).

Building codes around the globe do not currently incorporate information drawn from high-resolution dual-Doppler radar into their definition of wind profiles. Given the strong relationship between dual-Doppler radar and anemometric wind histories observed in Gunter et al. (2015), there does appear to be scope for this to occur. What is needed though, is a wider analysis of concomitant measurements so that theoretical or empirical relationships between dual-Doppler derived wind measurements can be readily compared with more traditional wind measurements and statistics. Thus, this paper presents preliminary comparisons between 0.4 Hz horizontal dual-Doppler wind speeds and equivalent (i.e. decimated) ultrasonic and UVW anemometric wind speeds collected during a convective thunderstorm outflow event at RTC on 4 June 2012. The work is being undertaken as an extension of the research conducted by Gunter et al. (2015) to develop empirical relationships between horizontal dual-Doppler radar and anemometric wind histories so these data can be used with confidence by the wind engineering community.

### Data and methods

Prior to making any comparison with the NWI 200-m tower anemometer data, TTUKa radar RHI sweep files had to be conditioned for dual-Doppler processing. This involved aligning the radar RHI sweep files in time so that the three-dimensional wind vector could be retrieved. For the purposes of this study, TTUKa-1 was assumed to be the reference radar and based on system clock calibrations, a six second offset had to be applied to TTUKa-2 records. After doing this, if the time difference between the two radar time stamps was less than or equal to two-seconds they were considered "aligned." A total of 3,785 of 4,418 TTUKa-1 RHI sweep files were matched with TTUKa-2 RHI sweep files. Time aligned TTUKa radar RHI sweep files were then processed using the quality control procedures outlined in Gunter et al. (2015) to account for velocity folding, noise, attenuation, and

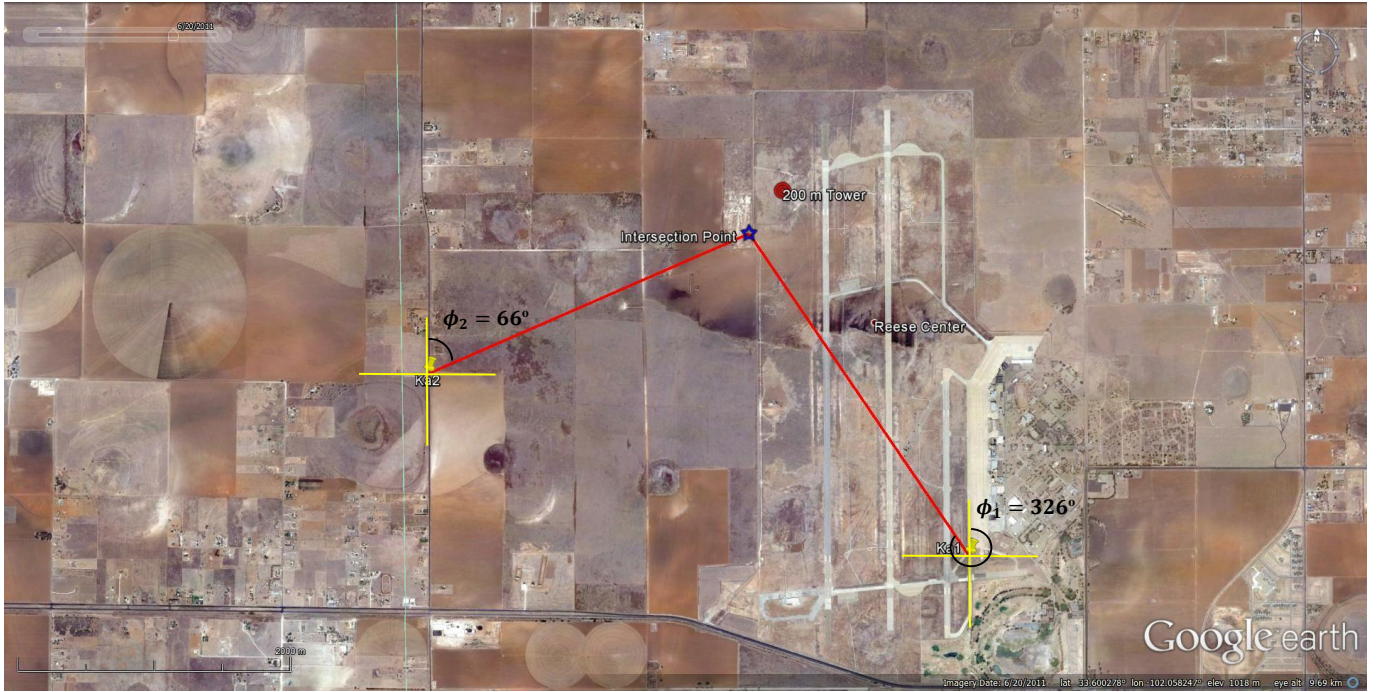


Fig. 1. TTUKa-band mobile Doppler radar deployment locations during the 4 June 2012 thunderstorm outflow event from Gunter et al. (2015). Yellow pins represent the locations of TTUKa-1 and TTUKa-2 respectively, the blue open star indicates the location of the intersection of each radar's RHI scans, where dual-Doppler horizontal wind profiles were generated, and the red bullseye represents the location of the NWI 200-m tower. The radar azimuth angles ( $\phi_1$  and  $\phi_2$ ) are also shown in a north aligned meteorological coordinate system.

signal processing jitter. A custom MATLAB script developed at Texas Tech University (TTU) was used to extract out the elevation angle, Doppler radial velocity, and height of the Doppler radial velocity measurement within the range bin closest to the intersection point of the two radars. The intersection of the RHI sweeps was computed using basic geometry in combination with the truck-relative bearing and position information logged during the deployment (Figure 1). The setup for the 4 June 2012 case discussed in this paper had an intersection point 391 m southwest from the NWI 200-m tower.

To account for sight differences in the RHI elevation angles between the two mobile radars, a vertical height binning grid with 20-m resolution was setup in a similar manner to Gunter et al. (2015). The mean elevation angles, Doppler radial velocities, and measurement heights were computed within each vertical height bin and assigned to the middle of the vertical height bins. The use of averaged elevation angles and Doppler radial velocities lead to some spatial averaging but was necessary.

To compute the horizontal dual-Doppler velocity at each grid point, the Doppler radial velocities from each radar were related to the east-west ( $u$ ) and north-south ( $v$ ) Cartesian wind components through the following equations:

$$V_{r1} = u \cos \phi_1 \sin \theta_1 + v \cos \phi_1 \sin \theta_1 + (w + V_t) \sin \phi_1, \quad (1)$$

$$V_{r2} = u \cos \phi_2 \sin \theta_2 + v \cos \phi_2 \sin \theta_2 + (w + V_t) \sin \phi_2, \quad (2)$$

where  $V_{r1}$  and  $V_{r2}$  are the vertical height bin averaged Doppler radial velocities ( $\text{ms}^{-1}$ ),  $\phi_1$  and  $\phi_2$  are the radar azimuth angles (degrees),  $\theta_1$  and  $\theta_2$  are the vertical height bin averaged elevation angles from TTUKa-1 and TTUKa-2 respectively (degrees),  $w$  is the vertical velocity ( $\text{ms}^{-1}$ ), and  $V_t$  the fall speed ( $\text{ms}^{-1}$ ) of the hydrometeor being measured (Raghaven 2003). The last term in Equations (1-2) is neglected given that the radar RHIs used here, and in Gunter et al. (2015), were shallow ( $< 6^\circ$ ).

Solving a system of equations for Equations (1-2), and neglecting the last term in each, results in:

$$u = \frac{1}{\sin(\phi_1 - \phi_2)} \left\{ V_{r1} \frac{\cos \phi_2}{\cos \theta_1} - V_{r2} \frac{\cos \phi_1}{\cos \theta_2} \right\}, \quad (3)$$

$$v = \frac{1}{\sin(\phi_1 - \phi_2)} \left\{ V_{r2} \frac{\sin \phi_1}{\cos \theta_2} - V_{r1} \frac{\sin \phi_2}{\cos \theta_1} \right\}. \quad (4)$$

Squaring Equations (3-4), summing the squares, and taking the square root of the summation results in the dual-Doppler radar horizontal wind speed for each vertical height bin. The wind direction in each vertical height bin was computed by converting the Cartesian  $u$  and  $v$  components into a north-relative meteorological coordinate system. An example of a horizontal dual-Doppler radar horizontal wind speed and direction profile from the 4 June 2013 event can be seen in Figure 2.

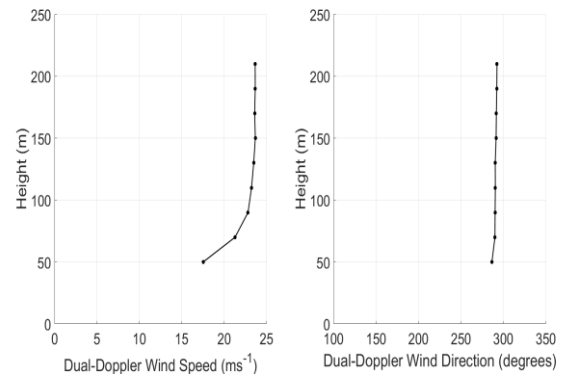


Fig. 2. 0.4 Hz dual-Doppler wind speed (left) and wind direction (right) generated at approximately 23:19:48 Z on 4 June 2012.

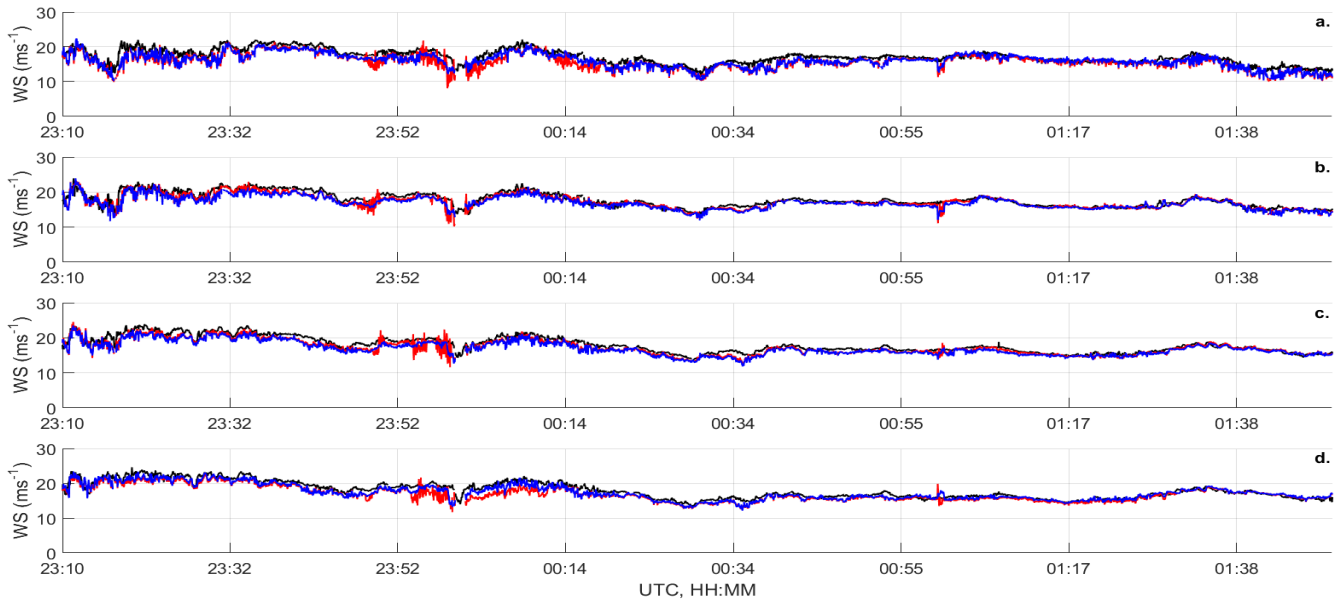


Fig. 3. Wind speed time history comparison between 0.4 Hz dual-Doppler radar (black), ultrasonic (red), and UVW (blue) wind speeds at approximately 50-m (a.), 70-m (b.), 110-m (c.), and 150-m (d.).

Ultrasonic and UVW 50 Hz anemometric records were screened using similar quality control techniques as Gunter et al. (2015) to remove spurious data points. Quality controlled ultrasonic and UVW wind data records were then decimated to the average dual-Doppler radar sampling frequency (0.4 Hz) using the instantaneous tower measurement closest to the time stamp of TTUKa-1, which again is considered to be the reference radar in this study.

### Preliminary comparisons

Preliminary comparisons between the dual-Doppler radar and decimated anemometric wind measurements were made at approximately 50-, 70-, 110-, and 150-m (Figures 3). Lower elevations (i.e. below 50-m) were excluded for this assessment due to an insufficient number of sample points in this region. Overall, the dual-Doppler radar horizontal wind speeds had a positive bias (i.e. dual-Doppler radar > anemometer) that ranges from  $0.51 \text{ ms}^{-1}$  to  $1.30 \text{ ms}^{-1}$  and was largest at 50-m. This represents biases of approximately 2.24% to 4.42% of the recorded mean wind speed. Neglecting the lag in time between dual-Doppler radar and anemometric wind histories (which exists due to the separation distance between the two), scatter plots of the decimated anemometric versus dual-Doppler radar horizontal wind speed were generated at each of the above mentioned heights. Data were segregated using Weather Surveillance Radar-1988 Doppler (WSR-88D) system reflectivity and radial velocity plan position indicator (PPI) scans (not shown) into two clusters: outflow (4-5 June ~23:10-00:14 UTC) and stratiform (5 June ~00:14-01:50 UTC). The outflow cluster was further segregated into 0.4 Hz dual-Doppler radar horizontal wind speeds  $\geq 19 \text{ ms}^{-1}$  and  $< 19 \text{ ms}^{-1}$ .

Linear regression was performed to determine an appropriate equation to relate the dual-Doppler radar horizontal wind speeds to anemometric wind speeds (Figure 4; ultrasonic not displayed). Regression model coefficients and fit statistics associated with each vertical height bin and regime compared in Figure 4 are shown in Tables 1-3. At first glance, the slope values in the outflow regime tend to be smaller in magnitude than for the stratiform regime. As height increases, the coefficient of determination,  $R^2$ , and root mean square error (RMSE) increase and decrease

respectively for the  $\geq 19 \text{ ms}^{-1}$  outflow regime, while  $R^2$  decreases for the  $< 19 \text{ ms}^{-1}$  outflow regime and RMSE generally decreases. The regression fit statistics deteriorate with increasing altitude for the  $< 19 \text{ ms}^{-1}$  outflow regime due to a decrease in the wind speed range and sample size with height. Another potential contribution to the poor explanatory power of the regression models is the large separation distance between the NWI 200-m tower and dual-Doppler radar RHI intersection point. For the stratiform regime,  $R^2$  and RMSE increased and decreased from 50-m, but do not vary significantly above said altitude.

Height (m)	Slope	Intercept	$R^2$	RMSE ( $\text{ms}^{-1}$ )	Count
50	0.76	3.05	0.18	1.25	680
70	0.79	2.96	0.32	1.03	993
110	0.87	1.19	0.59	0.88	1116
150	0.96	-0.27	0.66	0.90	1159

Table 1. Linear regression fit coefficients and statistics relating outflow ( $\geq 19 \text{ ms}^{-1}$ ) UVW and dual-Doppler radar horizontal wind speeds.

Height (m)	Slope	Intercept	$R^2$	RMSE ( $\text{ms}^{-1}$ )	Count
50	0.73	3.57	0.38	1.17	820
70	0.55	7.11	0.24	1.06	507
110	0.53	7.48	0.09	1.07	384
150	0.27	12.40	0.02	1.17	341

Table 2. Linear regression fit coefficients and statistics relating outflow ( $< 19 \text{ ms}^{-1}$ ) UVW and dual-Doppler radar horizontal wind speeds.

Height (m)	Slope	Intercept	$R^2$	RMSE ( $\text{ms}^{-1}$ )	Count
50	0.98	-0.58	0.61	1.07	2162
70	0.91	0.98	0.68	0.66	2158
110	0.86	1.54	0.63	0.65	2192
150	0.90	1.33	0.65	0.69	2188

Table 3. Linear regression fit coefficients and statistics relating post-outflow UVW wind speeds and dual-Doppler radar horizontal wind speeds.

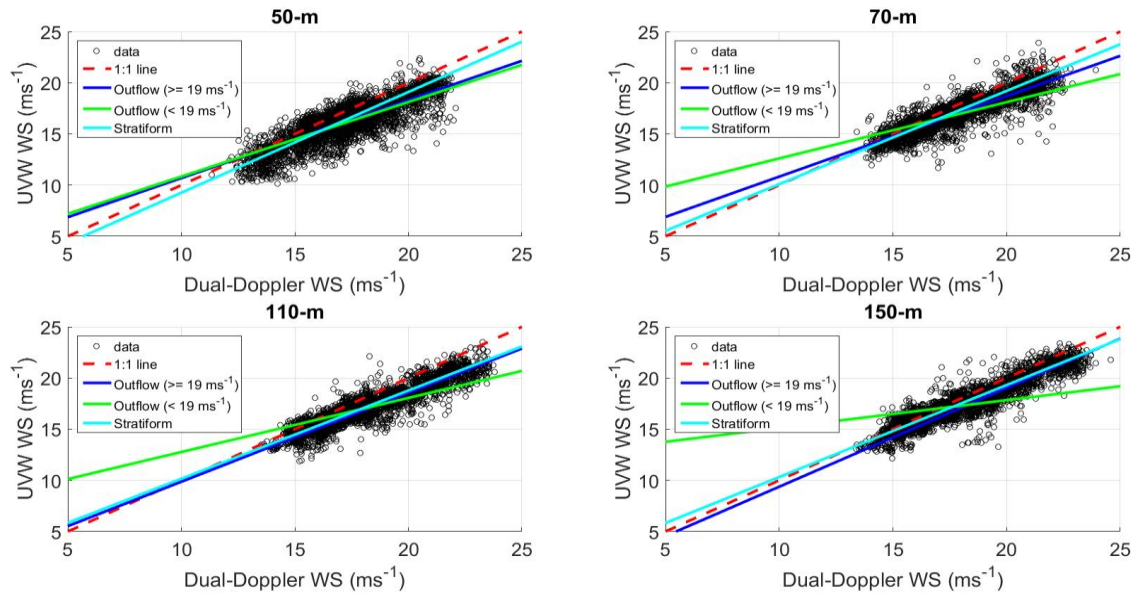


Fig. 4. Scatter plot of the decimated UVW versus dual-Doppler radar horizontal wind speed (open black circles) at average bin heights of 50-, 70-, 110- and 150- m. The dashed red, solid blue, solid green and solid cyan lines represent the 1:1 line and linear regression best fits to the outflow ( $\geq 19 \text{ ms}^{-1}$ ), outflow ( $< 19 \text{ ms}^{-1}$ ) and stratiform wind regimes, respectively.

## Discussion and future work

Using a newly introduced coordinated RHI radar scanning strategy created by Gunter et al. (2015), TTUKa dual-Doppler radar horizontal wind speed and direction measurements were generated and compared with 0.4 Hz ultrasonic and UVW anemometric wind records collected on the NWI 200-m tower. As noted by Gunter et al. (2015), dual-Doppler radar RHI horizontal wind speeds had a positive bias and the correlation between the dual-Doppler radar and ultrasonic/UVW wind speed measurements tended to increase with increasing height. Further examination of the dual-Doppler radar and anemometric wind histories revealed that there were time lags between the dual-Doppler radar and anemometric wind histories. The lack of temporal alignment was speculated to be due in part to the radar intersection point being over 300-m away from the NWI 200-m tower.

Linear regression models were fit to the 0.4 Hz UVW versus dual-Doppler radar horizontal wind speeds at approximately 50-, 70-, 110-, and 150-m in outflow ( $\geq 19 \text{ ms}^{-1}$  and  $< 19 \text{ ms}^{-1}$ ) and stratiform regimes. Results from the regression analysis showed that  $R^2$  increased and RMSE decreased with increasing altitude for the  $\geq 19 \text{ ms}^{-1}$  outflow regime and decreased and generally decreased respectively for the  $< 19 \text{ ms}^{-1}$  outflow regime. For the stratiform regime,  $R^2$  increased and RMSE decreased from 50-m, but did not vary significantly above 50-m. These results suggest that differences in the atmospheric conditions and dynamics play an important role in modulating the regression fits and warrant further examination.

Future work will include similar analysis of additional dual-Doppler radar-tower data sets collected closer to the NWI 200-m tower. Other data sets collected during the U.S. Department of Energy funded Experimental Measurement Campaign (XMC) for Planetary Boundary Layer (PBL) Instrument Assessment (XPIA) will also be obtained and analysed. All of these data sets will be used to further: 1.) evaluate the influence of separation distance on the correlation between dual Doppler radar RHI horizontal winds and anemometric wind histories, and 2.) determine an appropriate methodology to relate dual-Doppler radar horizontal wind measurements to anemometric wind histories.

Such a model will need to account for, at least, scatterer type, atmospheric conditions (i.e. clear air and snow), turbulence level within a radar sample volume and some measure of radar backscatter energy. How each of these influence the dual-Doppler radar RHI wind profile-anemometer relationship is not intuitive or straightforward. However, by developing a model to relate the two measurement platforms, the growing body of high-resolution mobile Doppler radar data can begin to be used to improve our understanding of outflow wind structure in a manner that is useable by the wind engineering community.

## Acknowledgments

Original funding for this research was supported by NSF Grant CMMI-1000160. Current work is funded through the Australian Research Council grant DE150101347. The authors would like to thank Jerry Guynes for designing, constructing, and maintenance of the TTUKa-band mobile Doppler radars, as well as, Dr. Stephen Morse for constructing and maintaining the 200-m tower database and initially processing the data used in this study.

## References

- Gunter, W. S., J. L. Schroeder, and B. D. Hirth (2015) Validation of Dual-Doppler Wind Profiles with in situ Anemometry. *Journal of Atmospheric and Oceanic Technology*, **32**, 943-960.
- Hirth, B. D., J. L. Schroeder, W. S. Gunter, and J. G. Guynes, (2015) Coupling Doppler radar-derived wind maps with operational turbine data to document wind farm complex flows. *Wind Energy*, **18**, 529-540.
- Raghaven, S. (2003) *Radar Meteorology*. Kluwer Academic Publishers, 549 pp.
- Weiss, C. C., J. L. Schroeder, J. Guynes, P. S. Skinner, and J. Beck (2009) The TTUKa mobile Doppler radar: Coordinated radar and in situ measurements of supercell thunderstorms during Project VORTEX2. 34th Conf. on Radar Meteorology, Williamsburg, VA, Amer. Meteor. Soc., 11B.